

PAPER

Impact of Spatial Diversity Reception on SAR Reduction in Implant Body Area Networks

Daisuke ANZAI^{†a)}, Member, Sho AOYAMA[†], Student Member, Masafumi YAMANAKA[†], Nonmember, and Jianqing WANG^{†b)}, Fellow

SUMMARY Wireless capsule endoscopy (WCE) is now one of most important applications in implant body area networks (BANs). WCE requires high throughput performance due to its real-time data transmission, whereas the communication performance depends much on the transmit power, which is strictly regulated in order to satisfy a safety guideline in terms of specific absorption rate (SAR). Spatial diversity reception is well known to improve the wireless performance without any temporal and spectral resource expansion. Additionally, applying spatial diversity reception to WCE systems can be expected to not only improve the wireless communication performance but also to reduce SAR. Therefore, this paper investigates the impact of spatial diversity reception on SAR levels for the 400 MHz medical implant communication service (MICS) band. To begin with, based on finite-difference time-domain (FDTD) simulations for implant BAN propagation with a numerical human body model, we first calculate the BER performance and derive the required transmit power to secure a permissible BER. Then, this paper calculates the local peak SAR under the required transmit power when the implant transmitter moves through the digestive organs. Finally, our simulation results demonstrate that applying spatial diversity reception can significantly reduce SAR in implant BANs.

key words: SAR, Implant BANs, WCE, Spatial diversity reception

1. Introduction

The concept of wireless body area networks (BANs) is becoming a reality due to recent breakthroughs in semiconductor technologies and wireless communications in recent years. Typical applications of wireless BANs include healthcare, medical treatment and medical monitoring [1]–[3]. BANs can be classified into two groups: wearable BANs and implant BANs. Wearable BANs are mainly used to monitor a person's health condition in daily life [2], whereas wireless capsule endoscopy (WCE) has been one of the most important applications in implant BANs [4], [5]. WCE involves the patient swallowing a small capsule, which contains a color camera, light source, battery and transmits images to the outside receiver in order to assist in diagnosing gastrointestinal conditions such as obscure malabsorption, gastrointestinal bleeding, chronic diarrhoea and abdominal pain. In this paper, we focus on WCE as an implant BAN application.

Since the human body may have high energy absorption in the microwave frequency band, it is necessary to sat-

isfy the regulation of specific absorption rate (SAR) which is an indicator of human safety. Therefore, we need to comply with the SAR safety guideline in realizing a wireless capsule endoscopy transmission. SAR is the amount of power absorbed per unit mass of human tissue. Since the implant transceiver of capsule endoscopy is very small, the induced SAR would be highly localized so that we only need to pay attention to the local peak SAR. According to the ICNIRP guideline [6], a local SAR as averaged over any ten grams should never exceed 2 W/kg (or 10 W/kg for occupational exposure). We therefore must satisfy the safety guideline at the same time of realizing a high reliability communication performance. However, the wireless communication performance strongly depends on the transmit power. This is because more transmit power leads to higher signal-to-noise power ratio (SNR) at a receiver side. Hence, it is important to evaluate the communication performance, i.e., bit error rate (BER) performance when the transmit power is limited by the safety guideline of SAR.

On the other hand, spatial diversity reception is well known as a technique to improve the wireless performance without any temporal and spectral resource expansion. Furthermore, in this paper, we pay attention to the feasibility that spatial diversity reception can not only improve the communication performance but also reduce SAR. As a spatial diversity reception technique, maximal-ratio combining (MRC) provides the best performance improvement in terms of maximizing the SNR, as compared with other combining techniques. However, MRC has the largest complexity of all combining techniques since it requires knowledge of channel state information (CSI) in each branch. From this viewpoint, equal gain combining (EGC) has an advantage in practice because it can be realized with less knowledge of CSI relative to the optimal MRC scheme [7]. Indeed, EGC usually does not require estimation of the channel fading amplitudes. Given this background, this paper focuses on EGC diversity reception.

In order to investigate the effect of spatial diversity reception on SAR reduction, we need to evaluate the transmit power to secure a permissible BER. For this purpose, the model of the propagation characteristics in the implant BANs at the 400 MHz medical implant communication service (MICS) band is required. Although several studies have so far been conducted to establish a path loss model for the capsule endoscopy [8], [9], no one has related it to the SAR. Therefore, this paper first performs a finite-difference time-

Manuscript received April 9, 2012.

Manuscript revised August 8, 2012.

[†]The authors are with Nagoya Institute Technology, Nagoya-shi, 466-8555 Japan.

a) E-mail: anzai@nitech.ac.jp

b) E-mail: wang@nitech.ac.jp

DOI: 10.1587/transcom.E95.B.3822

domain (FDTD) simulation for implant BAN propagation characteristic and local peak SAR calculation with a numerical human body model. In place of the difficulty in actual measurement of propagation characteristics for living humans, FDTD simulation has a merit to provide high-quality propagation data by using an anatomically based on high-resolution human body model [10]. Then, we derive an implant BAN channel model, and then calculate the BER performance under this implant propagation channel to determine the required transmit power for securing a permissible BER. Finally, we derive the local peak SAR and its statistical characteristic under the required transmit power. Such an approach can provide a threshold transmit power used to ensure that the local peak SAR never exceed the safety guideline.

The remaining of this paper is organized as follows. Section 2 presents the system model of the EGC diversity receiver. Then, Sect. 3 describes the implant propagation channel model for capsule endoscope, and Sect. 4 explains the SAR evaluation procedure under required BER performance. Next, Sect. 5 demonstrates and discusses the SAR evaluation results in the cases with and without the spatial diversity reception. Finally, Sect. 6 concludes this paper.

2. System Model for EGC Diversity Reception

We assume a transmitter with a single antenna inside a human body and an EGC diversity receiver with L antennas (branches) on the human body. Figure 1 shows the system model which is composed of an EGC diversity receiver with L diversity branches. The transmitter sends a signal $s(t)$, and we assume that the transmitter uses coherent BPSK modulation. The receiver is equipped with L diversity branches, hence the wireless channel is decomposed into L fading sub-channels. Defining the received signal at the l -th diversity branch as $r_l(t)$ ($l = 1, 2, \dots, L$), $r_l(t)$ is given by

$$r_l(t) = h_l(t) \otimes s(t) + n_l(t). \quad (1)$$

In Eq. (1), $h_l(t)$ and $n_l(t)$ denote the impulse response of the l -th sub-channel and the additive Gaussian noise at the l -th

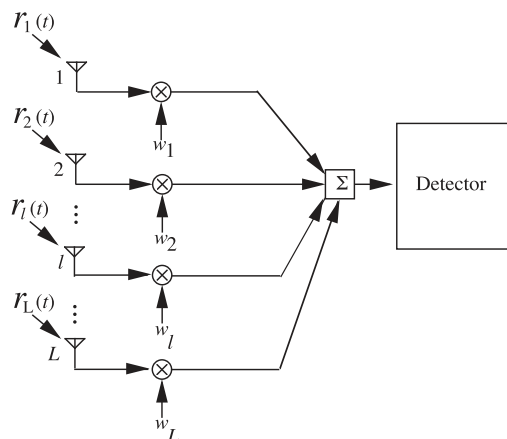


Fig. 1 Configuration of EGC diversity receiver.

diversity branch, respectively, and \otimes denotes the convolution. Here, we assumed that $n_1(t), n_2(t), \dots, n_L(t)$ are independent with the same power.

As shown in Fig. 1, the combined received signal $r(t)$ is represent as

$$r(t) = \sum_{l=1}^L w_l r_l(t) \quad (2)$$

where w_l denotes the diversity weight of the l -th branches. Since the EGC diversity receiver equally weighs them, the EGC diversity receiver obtains w_l as $e^{-j2\pi\theta_l}$, where θ_l is the phase of $h_l(t)$.

For equally likely transmitted symbols, it can be easily shown that the SNR at the output of the EGC combiner is given by

$$\gamma_{EGC} = \frac{(\sum_{l=1}^L |h_l(t)|)^2 \alpha^2}{\sum_{l=1}^L N_l} \quad (3)$$

where α and N_l are the amplitude of the transmitted signal and the power of the additive white Gaussian noise at the l -th branch, respectively.

3. Propagation Characteristics

We employed FDTD simulation to analyze the propagation characteristic and SAR. The employed numerical human body model, which was developed by National Institute of Information and Communication Technology, Japan [11], is shown in Fig. 2. The human body model is 1.73 m tall and 65 kg weight, and is composed of 51 kinds of biological tissues with a spatial resolution of 2 mm. Analyses based on the FDTD simulation with a numerical human body model have been so far performed in several papers, and the FDTD-based simulation results, including antenna characteristics, are validated by comparing with experimental results [12], [13]. The transmit antenna of capsule endoscope was assumed inside the digestive organs of the human body, and the receive antennas were placed at five locations on the body surface around the abdomen and back. In the FDTD simulation, a 4-mm long dipole as the transmit antenna was moved to have 30 locations inside the human body with three directivities as shown in Fig. 2, and the transmit antenna is covered with a 1 mm layer of air. The five receive antennas, denoted as in Fig. 3 with Rx_i ($i = 0, 1, \dots, 4$), were 20-mm long dipoles fixed in front of the body.

For the above-described simulation model, we calculated the received power at the seven receive antennas by using the FDTD method. Then, from the following equation

$$PL_{dB} = 10 \log_{10} \frac{P_t}{P_r} \quad (4)$$

where P_t and P_r are the transmit power and receive power, respectively, we obtained the instant path loss in unit of dB as a function of distance d between the transmitter and each

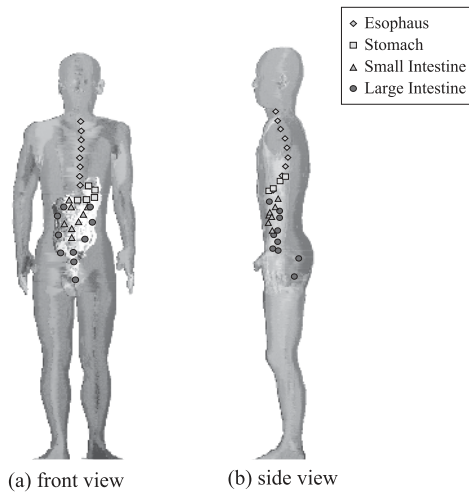


Fig. 2 Positions of capsule endoscope.

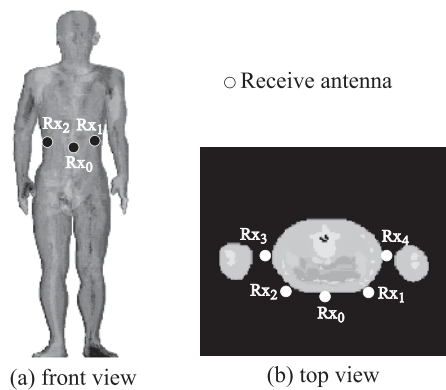


Fig. 3 Positions of receive antennas.

receiver. According to an empirical formula that the power decays in proportional to d^n , the average path loss $PL_{dB}^{average}$ can be expressed as

$$PL_{dB}^{average} = PL_{0,dB} + 10n \log_{10} \frac{d}{d_0} \quad (5)$$

where d_0 , $PL_{0,dB}$ and n are a reference distance, the path loss at the reference distance d_0 and the path loss exponent, respectively. Figure 4 shows an example of the path loss characteristic and a fitted curve given by (5) at the receive antenna of Rx_0 . The parameters in (5) were estimated by the least squares method. From this figure, we can see that the average path loss is well approximated by (5), and it is indeed proportional to d^n . Table 1 shows the fitted parameters in (5) for each receive antenna.

Next, we consider a shadowing effect caused by different organs surrounding the transmit antenna, namely, a shadow fading characteristic in the implant BAN channel. With the definition

$$S_{dB} = PL_{dB} - PL_{dB}^{average} \quad (6)$$

we have found that the statistical distribution of the shadow fading in decibel S_{dB} can be well approximated by normal

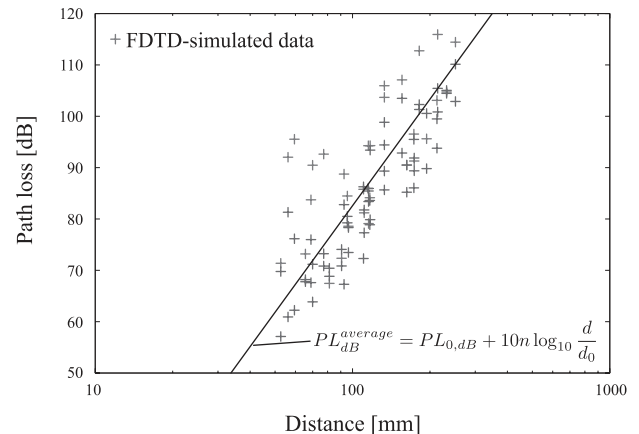


Fig. 4 Path loss characteristic.

Table 1 Fitted parameters of propagation characteristics.

	d_0 [m]	$PL_{0,dB}$	n	σ
Rx ₀	0.05	49.67	5.533	2.04
Rx ₁	0.05	37.81	5.997	2.20
Rx ₂	0.05	37.99	6.663	1.80
Rx ₃	0.1	59.74	6.421	2.17
Rx ₄	0.1	58.62	5.793	2.17

distribution [14]. That is to say, the lognormal distribution fits well the shadow fading data S at each receive antenna location. The probability density function (*pdf*) of lognormal distribution is given by

$$p(S) = \frac{1}{\sqrt{2\pi}\sigma S} \exp\left[-\frac{(\log S - \mu)^2}{2\sigma^2}\right] \quad (7)$$

where μ and σ denote the mean and standard deviation in log domain, respectively. From the definition in (6), the mean of S is zero, and the standard deviation is also shown in Table 1 for each receive antenna.

Finally, we explain correlation coefficients between received signals of two branches, which determine the communication performance of the spatial diversity reception. Let us define the correlation coefficient between the two received signals of Rx_l and Rx_k ($l, k = 0, 1, \dots, 4$) as

$$\rho_{l,k} = \frac{E[(r_l(t) - m_l)(r_k(t) - m_k)]}{\sqrt{E[(r_l(t) - m_l)^2]} \sqrt{E[(r_k(t) - m_k)^2]}} \quad (8)$$

$$m_l = E[r_l(t)] \quad (9)$$

where $r_l(t)$ and $E(\cdot)$ are the received signal at the l -th branch defined by Eq. (1) and the ensemble average of (\cdot) , respectively. In Table 2, we summarize the correlation coefficients $\rho_{l,k}$ based on the FDTD-simulated results. From this table, it is observed that the correlation coefficients range from 0.076 to 0.821, which suggests the feasibility of spatial diversity reception, if we adequately choose the receive antenna locations.

Table 2 Correlation coefficients between two received signals.

	Rx ₀	Rx ₁	Rx ₂	Rx ₃	Rx ₄
Rx ₀	–				
Rx ₁	0.399	–			
Rx ₂	0.306	0.692	–		
Rx ₃	0.076	0.209	0.594	–	
Rx ₄	0.399	0.821	0.524	0.219	–

4. SAR Evaluation Procedure under Required BER Performance

4.1 BER Performance Analysis

In order to derive the required transmit power to ensure a BER performance for capsule endoscope application, we need to calculate the BER performance of the EGC diversity reception under the derived implant shadow fading channel. Before describing the BER performance for the EGC spatial diversity reception ($L \geq 2$), this paper explains the BER performance of the single branch case ($L = 1$) at first. The average BER for the single branch case is calculated as

$$P_b^{single}(\bar{\gamma}) = \int_0^\infty P_b^{AWGN}(\gamma) p(\gamma|\bar{\gamma}) d\gamma \quad (10)$$

where $\bar{\gamma}$, $P_b^{AWGN}(\gamma)$ and $p(\gamma|\bar{\gamma})$ are the average SNR, the average BER under additive white Gaussian noise when the SNR is γ and the probability density function (pdf) on the SNR γ when $\bar{\gamma}$ is given, respectively. From (4) and (6), we obtain

$$\log S = -\log P_r + \log E[P_r]. \quad (11)$$

Taking into consideration that γ is expressed as P_r/N (also $\bar{\gamma}$ is expressed as $E[P_r]/N$) and S is Log-Normally distributed as shown in (7), $p(\gamma|\bar{\gamma})$ can be derived as

$$p(\gamma|\bar{\gamma}) = \frac{1}{\sqrt{2\pi\sigma\gamma}} \exp\left[-\frac{(\log \gamma - \log \bar{\gamma})^2}{2\sigma^2}\right]. \quad (12)$$

Now, assuming coherent demodulation of BPSK modulated signals, $P_b^{AWGN}(\gamma)$ is calculated as [15]

$$P_b^{AWGN}(\gamma) = \frac{1}{2} \operatorname{erfc}(\sqrt{\gamma}) \quad (13)$$

where $\operatorname{erfc}(\cdot)$ denote the complementary error function of (\cdot) .

Then, we derive the BER performance for the multiple branches case ($L \geq 2$). Defining the average SNR at each branch and the average SNR vector ($L \times 1$) as $\bar{\gamma}_l$ ($l = 1, \dots, L$) and $\bar{\Gamma} = [\bar{\gamma}_1, \dots, \bar{\gamma}_L]^T$, respectively, the average BER for the EGC diversity receiver is given by

$$P_b^{EGC}(\bar{\Gamma}) = \int_0^\infty P_b^{AWGN}(\gamma_{EGC}) p(\gamma_{EGC}|\bar{\Gamma}) d\gamma_{EGC}. \quad (14)$$

In the case of multiple branches ($L \geq 2$), we can not analytically derive the $p(\gamma_{EGC}|\bar{\Gamma})$. This is because γ_{EGC} is represented by Eq. (3), and as a result, γ_{EGC} includes the sum of

Table 3 Parameters for deriving transmit power from SNR.

T_0 [K]	296
B [MHz]	1
N_F [dB]	6
K	1.36×10^{-23}

Log-Normally distributed random variables ($|h_l(t)|$ in (3) is Log-Normally distributed), and furthermore, from Table 2, the received signals at all receive branches are uncorrelated with each other. Hence, we derive the $p(\gamma_{EGC}|\bar{\Gamma})$ by a numerical analysis based on Monte Carlo simulation (a theoretical analysis of the BER performance is our future work).

4.2 Calculation of Required Transmit Power and SAR

Next, we link the SNR and the transmit power. Let us assume that the only noise source at the receiver is AWGN. This noise is typically thermal, introduced by the receive antenna and the front-end circuit of the receiver. The thermal noise power is given by

$$N = kT_0BN_F \quad (15)$$

where k , T_0 , B and N_F denote the Boltzmann constant, the environment temperature, the communication bandwidth or data rate and the noise figure of receiving device, respectively. Then, the transmit power can be calculated as

$$\begin{aligned} P_{t,dBW} &= P_{r,dBW} + PL_{dB} \\ &= \gamma_{dB} + 10 \log_{10}[kT_0B] + N_{F,dB} + PL_{dB}. \end{aligned} \quad (16)$$

Table 3 gives the parameters for deriving the transmit power from the SNR γ_{dB} . As mentioned in the previous section, we employ a 4-mm long dipole as the transmit antenna and a 20-mm long dipoles as the receive antennas for the 400 MHz MICS band signal, therefore, antenna matching cannot be achieved anymore. In this paper, to evaluate a realistic transmitted power, we calculate the attenuation caused by this antenna mismatch based on the FDTD simulation, and introduce it into the path loss effect PL_{dB} . As for an evaluation criterion of the BER performance, it is set to 10^{-3} . This is because the BER before forward error correction (FEC), namely, channel BER of around 10^{-3} is required in order to achieve that the BER after FEC becomes error free [16]. For example, Fig. 5 shows the average transmit power versus the BER performance for the case of the two branches of Rx₀ and Rx₁, where we used the parameters of the propagation characteristics shown in Table 1. Moreover, for comparison purpose, the figure also includes the result for the single branch case at Rx₀ and Rx₁. This figure suggests that, in the case of two diversity branches of Rx₀ and Rx₁, a transmit power of around -1 dBm is required to ensure a BER of 10^{-3} .

On the other hand, the safety to human body is evaluated in terms of the SAR as averaged over any ten gram of tissue. The SAR is expressed as

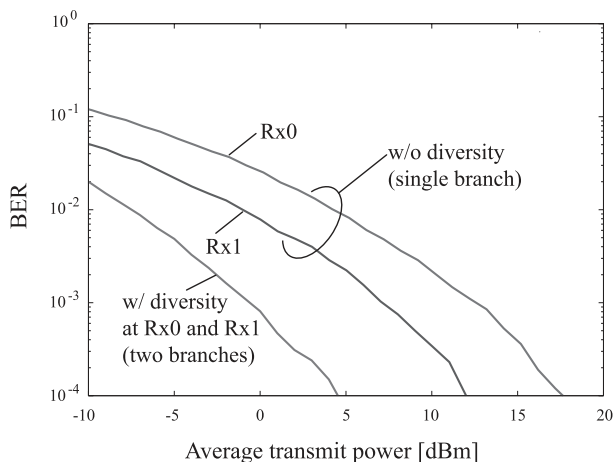


Fig. 5 BER performance versus average transmit power.

$$SAR = \frac{\sigma}{\rho} E^2. \quad (17)$$

In (17), σ , ρ and E are the conductivity of tissue, the mass density of tissue and the electric field rms value inside tissue, respectively. To calculate the SAR, we employ FDTD simulation with the numerical human model shown in the Sect. 3. The transmit power of the capsule endoscope is determined based on the above procedure for ensuring a BER of 10^{-3} . As mentioned previously, the ICNIRP safety guideline requires 2 W/kg (or 10 W/kg for occupational exposure) to be satisfied. Note that this safety guideline of 2 W/kg (or 10 W/kg) assumes that a transmission source exists outside a human body, however, to the best authors' knowledge, the safety guideline which assumes that it exists inside a human body has been not established yet. Therefore, unfortunately, we have no choice but to apply the safety guideline of 2 W/kg (or 10 W/kg) in this paper (applying an appreciate safety guideline to SAR evaluation in a capsule endoscopy system is our future work).

5. SAR Evaluation Results

5.1 Simulation Scenario without Spatial Diversity Reception (Single Branch Case)

First, we demonstrate the results for the case of a single branch, namely, no spatial diversity reception case. To begin with, the required transmit power was calculated. Table 4 shows the required transmit power for obtaining an average BER of 10^{-3} , and the required transmit power for obtaining a BER always below 10^{-3} , respectively. We name the transmit power in the former case as the required average transmit power and that in the latter case as the required maximum transmit power. We can see that the average and maximum transmit powers are different at different receiver locations. Note that the all average transmit powers, except for Rx₀ and Rx₃, are smaller than 10 mW, and such a transmit power can never induce a 10-gram average SAR exceeding 2 W/kg, that is, in this sense, the safety guideline is satis-

Table 4 Average and maximum transmit power at BER = 10^{-3} in the case without spatial diversity reception.

	Maximum transmit power [mW]	Average transmit power [mW]
Rx ₀	120.71	20.85
Rx ₁	52.04	5.04
Rx ₂	20.83	2.96
Rx ₃	115.10	18.25
Rx ₄	105.12	7.70

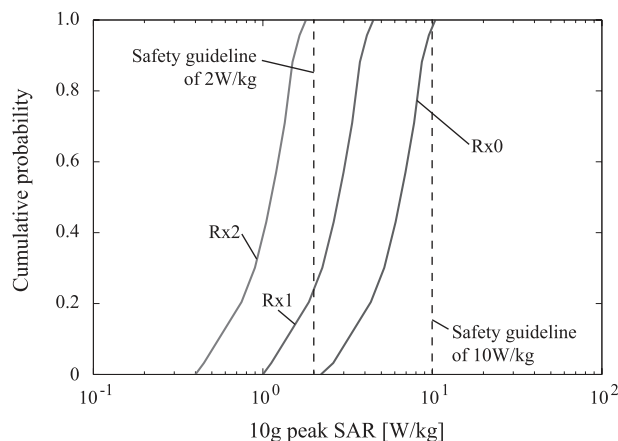


Fig. 6 Cumulative probability of 10g peak SAR in the case without spatial diversity reception.

fied. However, if we require a higher communication quality to ensure the BER smaller than 10^{-3} in any capsule location, the SAR will be determined by the maximum transmit power in Table 4.

Figure 6 shows the cumulative probabilities of the 10-gram average peak SARs when the transmit antenna moves along the digestive organs to have the 30 locations and three different directivities. The SAR values were calculated at the maximum transmit power for Rx₀, Rx₁ and Rx₂, respectively. As can be seen, if the receive antenna is set at Rx₂ location, a transmit power of 20.83 mW is required to ensure a BER not exceeding 10^{-3} . Such a transmit power yields a local peak SAR ranging from 0.4 to 1.8 W/kg, that do not exceed the safety guideline of 2 W/kg. On the other hand, if the receive antenna is set at Rx₁ location, a transmit power of 52.04 mW is required to ensure a BER not exceeding 10^{-3} . In this case, the local peak SAR may exceed the 2 W/kg at about 80% of the all transmitter locations, and furthermore, in view of that the capsule endoscope is medical treatment, it should be acceptable to use the 10 W/kg as the safety guideline. Therefore, in this means, the induced local peak SAR is still satisfied. However, unfortunately, if the receive antenna is set at Rx₀, a transmit power of 120.71 mW is required, and we can see from Fig. 6 that even the safety guideline of 10 W/kg can not be satisfied any more. Consequently, the results in Fig. 6 also suggest that the SAR is dependent on the receive antenna locations, as a result, we have concluded that the receive antenna location should be carefully considered to comply the safety guideline. If we

Table 5 Average transmit power at BER = 10⁻³ in the case with spatial diversity reception.

	Average transmit power [mW]				
	Rx ₀	Rx ₁	Rx ₂	Rx ₃	Rx ₄
Rx ₀	–				
Rx ₁	0.85	–			
Rx ₂	0.70	0.35	–		
Rx ₃	1.50	0.70	0.60	–	
Rx ₄	1.05	0.55	0.42	0.90	–

Table 6 Maximum transmit power at BER = 10⁻³ in the case with spatial diversity reception.

	Maximum transmit power [mW]				
	Rx ₀	Rx ₁	Rx ₂	Rx ₃	Rx ₄
Rx ₀	–				
Rx ₁	2.99	–			
Rx ₂	1.58	1.54	–		
Rx ₃	2.98	2.71	1.49	–	
Rx ₄	5.19	5.08	2.54	4.81	–

can optimally choose a receiver location, for example Rx₂, both the BER smaller than 10⁻³ and the local SAR smaller than 2 W/kg are securable.

5.2 Simulation Scenario with Spatial Diversity Reception (Multiple Branches Case)

Next, this paper shows the results for the case of multiple branches, and investigates the effect of spatial diversity reception on SAR reduction. In this paper, we consider only the case of two branches ($L = 2$), however, the SAR evaluation for the case of more than three branches ($L \geq 3$) can be realized by the similar way in the case of two branches. In the same similar way to the single branch case, the required transmit power for the case with the spatial diversity reception was calculated at first. Tables 5 and 6 show the required average transmit power and the required maximum transmit power, respectively. As compared with the results for the case without spatial diversity reception in Table 4, we can see that applying spatial diversity reception to the receivers can significantly reduce both the required average and maximum transmit powers. Furthermore, the required average transmit power is always less than 10 mW at all selections of the receive antennas, namely, the 10-gram average SAR exceeding 2 W/kg can not occur. Additionally, our guess is that the required transmit power may be determined by both the two effects of the path loss and the correlation coefficient. In order to optimally choose the diversity branches, it is important to take consideration into the both the two effects. If we can choose the best receive antenna positions, for example Rx₂ and Rx₃, the achievable required maximum transmit power is 1.49 mW, and it is around 6% of 20.83 mW, which is the minimum value in the case without the spatial diversity reception.

Figure 7 shows the cumulative probabilities of the 10-gram average peak SARs in the case with the spatial diversity reception at the required maximum transmit powers for the best selection (Rx₂ and Rx₃) and the worst selection

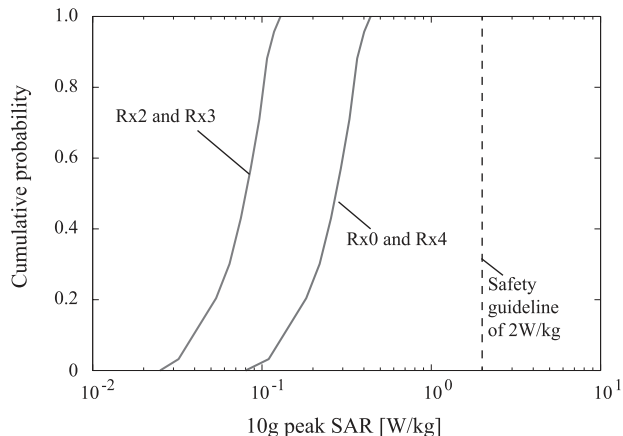


Fig. 7 Cumulative probability of 10g peak SAR in the case with spatial diversity reception.

Table 7 Threshold transmit power at a local peak SAR.

Local peak SAR [W/kg]	Transmit power [mW]
2	24.36
10	121.80

(Rx₀ and Rx₄). From this figure, in addition to the required transmit power, the SARs are also remarkably reduced as compared with those for the single branch case. Even if the two receive antennas are set to Rx₀ and Rx₄ (the worst selection), a transmit power of only 5.19 mW is required to ensure a BER not exceeding 10⁻³. This result means that the maximum transmit powers for the case with the spatial diversity reception can never exceed 2 W/kg. Moreover, if we can optimally select the diversity branches, for example the selection of Rx₂ and Rx₃, the 10-gram average SAR has 10 times safety margin of the safety guideline of 2 W/kg.

In addition, Table 7 gives the permissible transmit power for securing the local SAR not exceeding 2 W/kg or 10 W/kg, that can be used as a threshold transmit power in safety evaluation for capsule endoscope transceiver with the spatial diversity reception. Then, our future subject is that we insert an implant transceiver into a liquid phantom of human body and measure its transmit power. By comparing the measured transmit power with the threshold transmit power, it is possible to evaluate the safety of the transceiver for capsule endoscope application.

6. Conclusion

This paper has investigated the impact of spatial diversity reception on SAR reduction in implant BANs. In order to evaluate the transmission performance and the local peak SAR in a WCE scenario, we have performed FDTD simulations using a numerical human body model in the 400 MHz MICS band. Based on the simulation results, we have derived an implant shadow fading channel model, and then calculated the BER performance of the EGC diversity receiver under the derived channel.

As a result, in the case without the spatial diversity re-

ception (the single branch case), we have found that the required transmit power is 52.04 mW for securing a BER below 10^{-3} when the receiver antenna is located at Rx_1 . Under this transmit power, the 10-gram local peak SAR has been shown to exceed the safety guideline of 2 W/kg, although not exceed 10 W/kg, in some transmitter locations inside the digestive organs, that is, if we choose the worst receive antenna location, even the safety guideline of 10 W/kg can not be satisfied.

On the other hand, in the case with the spatial diversity reception (two branches case), we have seen from the numerical analyses that the required average power is less than 10 mW at all selections of the receive antennas, that is, the 10-gram average SAR exceeding 2 W/kg will never be induced. In a reality, it is difficult to know the optimum receive antenna position in advance, so we can not always choose the optimum position. However, even if the worst positions are chosen, the safety guideline of 2 W/kg can be satisfied in the case of the spatial diversity reception, whereas the safety guideline of 10 W/kg cannot be satisfied in the case without the spatial diversity reception. In this situation, the proposed SAR reduction by using the spatial diversity reception is necessary to satisfy the safety guideline. Furthermore, because a capsule endoscope is driven only by battery, the spatial diversity reception is advantageous in terms of the lower required transmitted power. In addition, by choosing the best receive antenna locations, for example Rx_2 and Rx_3 , the achievable required maximum transmit power is 1.49 mW, which is around 6% of the minimum value of 20.83 mW for the case without the spatial diversity reception. In this case, we have also confirmed that the 10-gram average SAR has 10 times safety margin of the safety guideline of 2 W/kg.

Acknowledgment

This study was supported partially by Telecom Engineering Center, Japan and JSPS KAKENHI Grant Number 24560452.

References

- [1] H.B. Li and R. Kohno, "Body area network and its standardization at IEEE 802.15. BAN," *Advances in Mobile and Wireless Communications*, pp.223–238, 2008.
- [2] E. Monton, J.F. Hernandez, J.M. Blasco, T. Herve, J. Micallef, I. Grech, A. Brincat, and V. Traver, "Body area network for wireless patient monitoring," *IET Commun.*, vol.2, no.2, pp.215–222, Feb. 2008.
- [3] V. Leonov, P. Fiorini, S. Sedky, T. Torfs, and C. Van Hoof, "Thermoelectric MEMS generators as a power supply for a body area network," *Proc. IEEE Solid-State Sensors, Actuators and Microsystems 2005*, vol.1, pp.291–294, June 2005.
- [4] G. Iddan, G. Meron, A. Glukhovsky, and P. Swain, "Wireless capsule endoscopy," *Nature*, vol.405, p.417, May 2000.
- [5] G. Costamagna, S.K. Shah, M.E. Riccioni, F. Foschia, M. Mutignani, V. Perri, A. Vecchioli, M.G. Brizi, A. Picciocchi, and P. Marano, "A prospective trial comparing small bowel radiographs and video capsule endoscopy for suspected small bowel disease," *Gastroenterology*, vol.123, no.4, pp.999–1005, Oct. 2002.
- [6] ICNIRP, "Guidelines for limiting exposure to time-varying electric, magnetic and electromagnetic fields (up to 300 GHz)," *Health Physics*, vol.74, pp.494–522, 1998.
- [7] A. Annamalai, C. Tellambura, and V.K. Bhargava, "Equal-gain diversity receiver performance in wireless channels," *IEEE Trans. Commun.*, vol.48, no.10, pp.1732–1745, Oct. 2000.
- [8] T. Aoyagi, K. Takizawa, T. Kobayashi, J. Takada, K. Hamaguchi, and R. Kohno, "Development of an implantable WBAN path-loss model for capsule endoscopy," *IEICE Trans. Commun.*, vol.E93-B, no.4, pp.846–849, April 2010.
- [9] K. Sayrafian-Pour, W. Yang, J. Hagedorn, J. Terrill, and K.Y. Yazdandoost, "A statistical path loss model for medical implant communication channels," *Proc. IEEE PIMRC 2009*, pp.2995–2999, Sept. 2009.
- [10] J. Wang, Y. Nishikawa, and T. Shibata, "Analysis of on-body transmission mechanism and characteristic based on an electromagnetic field approach," *IEEE Trans. Microw. Theory Tech.*, vol.57, no.10, pp.2464–2470, Oct. 2009.
- [11] T. Nagaoka, S. Watanabe, K. Sakurai, E. Kunieda, S. Watanabe, M. Taki, and Y. Yamanaka, "Development of realistic high-resolution whole-body voxel models of Japanese adult males and females of average height and weight, and application of models to radio-frequency electromagnetic-field dosimetry," *Phys. Med. Biol.*, vol.49, pp.1–15, Jan. 2004.
- [12] J. Wang, O. Fujiwara, S. Kodera, and S. Watanabe, "FDTD calculation of whole-body average SAR in adult and child models for frequencies from 30 MHz to 3 GHz," *Phys. Med. Biol.*, vol.51, no.17, pp.4119–4127, Aug. 2006.
- [13] J. Wiart, A. Hadjem, M.F. Wong, and I. Bloch, "Analysis of RF exposure in the head tissues of children and adults," *Phys. Med. Biol.*, vol.53, no.13, pp.3681–3695, June 2008.
- [14] D. Anzai, S. Aoyama, and J. Wang, "Performance analysis on equal gain combining diversity receiver for implant body area networks," *Proc. 4th Int. Symp. on Applied Science in Biomedical and Commun. Tech. (ISABEL)*, in CD-ROM, Oct. 2011.
- [15] J.G. Proakis and M. Salehi, *Digital Communications*, McGraw-Hill, 2008.
- [16] R. Mehmood, E. Cerqueira, R. Piesiewicz, I. Chlamtac, *Communications Infrastructure, Systems and Applications*, Springer-Verlag New York, 2010.



Daisuke Anzai received the B.E., M.E. and Ph.D. degrees from Osaka City University, Osaka, Japan in 2006, 2008 and 2011, respectively. Since April 2011, he has been an Assistant Professor at the Graduate School of Engineering, Nagoya Institute of Technology, Nagoya, Japan. He has engaged in the research of biomedical communication systems and localization systems in wireless communication networks.



Sho Aoyama was born in Aichi, Japan, in 1989. He received the B.Eng. degree from Nagoya Institute of Technology, Aichi, Japan in 2011. He is currently pursuing the M.Eng. course at Nagoya Institute of Technology, engaging in the research on wireless communication in body area networks.



Masafumi Yamanaka was born in Gifu, Japan, in 1990. He received the B.Eng. degree from Nagoya Institute of Technology, Aichi, Japan in 2012. He is currently pursuing the M.Eng. course at Nagoya Institute of Technology, engaging in the research on biological electromagnetic compatibility.



Jianqing Wang received the B.E. degree in electronic engineering from Beijing Institute of Technology, Beijing, China, in 1984, and the M.E. and D.E. degrees in electrical and communication engineering from Tohoku University, Sendai, Japan, in 1988 and 1991, respectively. He was a Research Associate at Tohoku University and a Senior Engineer at Sophia Systems Co., Ltd., prior to joining the Nagoya Institute of Technology, Nagoya, Japan, in 1997, where he is currently a Professor. His research interests include biomedical communications and electromagnetic compatibility.